Optical response functions for condensed systems with linear and quadratic electron–vibration coupling

Mohamad Toutounji and Gerald J. Small[a)]
Department of Chemistry, Iowa State University, Ames, Iowa 50011

Shaul Mukamel
Department of Chemistry, University of Rochester, Rochester, New York 14627

(Received 7 May 1998; accepted 7 August 1998)

Understanding the similarities and differences between optical coherence loss of electronic transitions of chromophores in glasses and in the glass forming solvent requires, in part, linear response (2-point correlation) functions, $J(t;T)$. An approximate excited state vibrational Hamiltonian (H_e) which accounts for both linear and quadratic electron–phonon coupling is derived that is acceptable for mode frequency changes smaller than 30%. The associated linear response function for the case of no damping is obtained. A response function that includes damping is proposed for systems whose modes are either linearly or quadratically coupled. It is the product of three response functions, two of which are phononic and associated with linear and quadratic modes. The third response function is electronic with a dephasing frequency γ_{el} that is the width of the zero-phonon line. The total response function yields single-site absorption spectra in which folding of the widths of multi-phonon and sequence transitions occurs. Applications of the new response functions are made to the temperature dependence of single-site absorption and hole-burned spectra of the special pair band of the bacterial reaction center and the temperature dependence of the single site absorption spectrum of Al-phthalocyanine tetrasulphonate in glassy ethanol. © *1998 American Institute of Physics.* [S0021-9606(98)70942-0]

I. INTRODUCTION

Recently, there has been considerable activity in the use of femtosecond photon echo spectroscopies to study how nuclear (vibrational) motions lead to the coherence loss of optical transitions of solute chromophores in liquids at room temperature.[1–12] Of particular interest has been the role of inertial (librational) intermolecular modes (''phonons'') which couple linearly to the electronic transition and lead to optical dephasing on a timescale shorter than 1 ps. (Such modes lead to multi-phonon transitions in the $S_1 \leftarrow S_0$ absorption spectrum.) One reason for this interest is that the inertial modes may set the stage for longer timescale, larger amplitude nuclear solvent dynamics which are the rate limiting step in condensed phase electron–transfer reactions. The multimode Brownian oscillator (MBO) model[13–15] has often been used in the interpretation of the data. In this model the linearly coupled modes are the primary BOs which, along with the bath oscillators, are taken to be harmonic. The coupling between a primary BO and the bath modes is linear in the BO displacement which results from electronic excitation of the chromophore. This coupling gives rise to a damping constant, $\gamma_j(\omega)$, for BO j of frequency ω_j. This gives rise to an effective frequency-dependent damping ($\gamma_j(\omega_j)$) for the jth BO where the frequency dependence arises from the spectral distribution of the BO's coupling to the bath oscillators. $\gamma_j(\omega)$ enters into the optical response function (see p. 227 of Ref. 15). In applications of the MBO model the frequency dependence of γ_j is commonly neglected which amounts to a white spectrum for the bath (known as Ohmic dissipation). In the case of an underdamped mode ($\gamma_j < \omega_j$), this leads to a width for the zero-phonon line (ZPL) of $2S_j(2\overline{n_j}+1)\gamma_j$, where S_j is the Huang–Rhys factor and $\overline{n_j}$ the thermal occupation number of BO j. Only when the frequency dependence of γ_j is properly taken into account does $\gamma_j(\omega)$ vanish as $\omega \rightarrow 0$ so that the phononic relaxation does not contribute to the width of the ZPL, as should be the case. In addition, it would be necessary to combine the standard MBO model with other models for electronic dephasing (*vide infra*) since it does not account for such dephasing. Work in this direction is in progress.

As discussed in Refs. 16, 17, hole burning and photon echo spectroscopies have been used to study pure electronic dephasing of the ZPL of chromophores in glasses and polymers at low temperatures since the early 1980s (see Refs. 18, 19 for reviews). At temperatures lower than about 10 K the homogeneous width of the ZPL is determined by the tunneling dynamics of the bistable configurations or two-level systems of the glass. Above about 15 K the dephasing is dominated by quadratic electron–phonon coupling of the type identified earlier for chromophores in host crystals. The studies of the ZPL in glasses and polymers led to three important findings. The first is that the exchange coupling dephasing mechanism,[20,21] which stems from diagonal quadratic electron–phonon coupling, often accounts for the homogeneous width of the ZPL at higher temperatures. This coupling leads to a change in the frequency of a pseudo-

a)Electronic mail: gsmall@ameslab.gov

localized phonon upon electronic excitation of the chromophore. The second finding is that these dephasing phonons are Franck–Condon (FC) inactive, i.e., exhibit negligible linear electron–phonon coupling. The third finding is that the linearly coupled modes responsible for multi-phonon transitions appear to be infrequently involved in pure electronic dephasing. The last two findings suggest that the system phonons can often be divided into two subsets, one associated with linear coupling and the other with quadratic coupling. The most detailed studies which support the above findings involved spectral hole burning experiments on Alphthalocyanine tetrasulphonate (APT) in hyperquenched glassy films of water,[16] ethanol and methanol[17] which were performed over a very wide temperature range, 5–~130 K. In the case of water, the exchange coupling modes correlated with the 50 and 180 cm^{-1} transverse and longitudinal acoustic modes of liquid water. For ethanol, the exchange coupling mode frequency is ~50 cm^{-1}, close to the first maximum in the spectral density of liquid ethanol. High resolution hole-burned spectra proved that these modes exhibit little if any FC activity. For water, ethanol and methanol the FC activity by intermolecular modes is dominated by phonons at 38, 26 and 17 cm^{-1}, respectively. They were assigned as modes mainly associated with APT librational motion. In the case of glassy water, characterization and determination of the electron–phonon coupling parameters (including the Huang–Rhys factor and shape of the one-phonon profile for the linearly coupled mode at 38 cm^{-1}) and static inhomogeneous broadening associated with the pure electronic transition at lower temperatures led to calculated hole-burned spectra for higher temperatures in good agreement with the experimental spectra.[16] The frequency domain hole burning theory of Hayes *et al.*[22–24] was used for the calculations. The results indicate that the above inhomogeneous broadening is constant over the temperature range used in the experiments. Given the good agreement, the same experimentally determined parameters were used to calculate the width of the APT's origin absorption band in water at room temperature. The value of 500 cm^{-1} obtained differs by only 10 cm^{-1} from the experimental value. It was suggested that the combination of temperature dependent hole burning and photon echo studies above and below the glass transition of the solvent should provide new insights on optical coherence loss of chromophores in liquids (see also Refs. 25, 26).

We present here linear response or 2-point correlation functions, $J(t;T)$, which do yield single-site absorption and hole-burned spectra at finite temperature that describe the essential features of experimental spectra. (The harmonic approximation is assumed for the optically active modes.) The response functions are appropriate for modes which are underdamped, $\gamma_j < \omega_j$.[27] The cases of critically damped and overdamped modes are treated in Chap. 8 of Ref. 15. The case of linear electron–phonon coupling is considered first. The form of $J(t;T)$ yields, for example, widths (fwhm) of $\gamma_{el}(T)+n_j\gamma_j(T)$ for members of the cold absorption progression ($n_j=0,1,...$) associated with mode j with $\gamma_{el}(T)$ the contribution from pure electronic dephasing. The linear dependence (folding) on n_j is valid for any relaxation mechanism of the active phonon that is linear in its coordinate. Insofar as the temperature dependencies of γ_{el} and γ_j are concerned, one need consider different mechanisms and feed their T-dependencies into $J(t;T)$, which is standard procedure. $J(t;T)$ or, equivalently the lineshape function $g(t;T)$, allows for straightforward evaluation of the 4- and higher-point correlation functions associated with photon echo spectroscopies. Next, we consider the case where the active modes exhibit diagonal quadratic electron–phonon coupling which results in mode frequency changes upon electronic excitation of the chromophore. An approximate excited state vibrational Hamiltonian, H_e, is derived which is shown to be adequate for a mode frequency change smaller than about 30%. (Off-diagonal quadratic electron–phonon coupling or the Duschinsky effect is neglected since it is expected to be unimportant for strongly allowed electronic transitions of dye molecules.[28] Such a change may be considered to be large for low frequency modes of condensed phase systems. An expression for the linear response function is derived for the case of no damping. A linear response function with damping is given for a system whose modes are either linearly or quadratically coupled (see the preceding paragraph for motivation). The response function is the product of three response functions, two of which are associated with a phononic contribution, one from linearly coupled modes and the other from quadratically coupled modes. The third response function is associated with pure electronic dephasing.

Applications of the new response functions include the single-site absorption and hole-burned spectra of the special pair band of the bacterial reaction center which previous studies had shown to be characterized by linearly coupled modes at 30 and 120 cm^{-1} (Ref. 29) and the temperature dependence of the single-site absorption spectrum of Alphthalocyanine tetrasulphonate in glassy ethanol.

II. THEORY AND CALCULATED SPECTRA

A. Approximate excited state vibrational Hamiltonian H_e and linear response function $J(t;T)$ with no damping

Consider absorption from the ground electronic state (g) to an excited electronic state (e) and let ω'' and ω' be, respectively, the ground and excited state frequencies of a vibrational mode. Let q be the dimensionless normal coordinate of this mode for the ground electronic state. It is related to the mass-weighted coordinate, Q, by $q=(\omega''/\hbar)^{1/2}Q$. Similarly, we define d as the dimensionless translational displacement between the potential energy minima of the two electronic states. For linear and diagonal quadratic electron–phonon coupling the excited state vibrational Hamiltonian is given exactly by[30]

$$H_e = H_g + \frac{\hbar\omega''}{2}\left[(r^2-1)q^2 + 2r^2qd + r^2d^2\right] + \hbar\Omega, \quad (1)$$

where $r=(\omega'/\omega'')$. $\hbar\Omega$ is the adiabatic electronic energy gap. The r^2d^2 term multiplied by $\hbar\omega''/2$ is the optical reorganization energy. Thus,

$$\Omega_v = \Omega + \omega'' r^2 d^2/2, \quad (2)$$

where Ω_v is the vertical (Condon) frequency gap. When $\omega' = \omega''$, the optical reorganization energy is $S\omega''$, with $S = d^2/2$ being the familiar Huang–Rhys factor. In Eq. (1), H_g is the vibrational Hamiltonian for the ground state:

$$H_g = \hbar\omega''(a^+ a + 1/2), \tag{3}$$

with a^+ and a the raising and lowering operators for the ground state, i.e., $q = 2^{-1/2}(a^+ + a)$. For a multimode system one need only sum Eq. (1) over all modes. When dealing with fluorescence or resonance Raman, one should interchange e and g, ω' and ω'' and associate q with the normal coordinate of the excited state [e.g., d would now equal $(\omega'/\hbar)\Delta Q$ rather than $(\omega''/\hbar)\Delta Q$]. The reader is referred to Ref. 31 for a further (and simple) discussion.

Exact solutions to the problem of determining the Franck–Condon factors associated with Eq. (1) have been available for many years.[32–35] Thus, the calculation of ''stick'' linear absorption spectra, $\sigma(\omega)$, is routine. One can introduce shapes to the sticks and calculate the temperature dependencies of the integrated absorption intensities of the vibronic (phononic) transitions. However, doing the equivalent of this in the time domain with Eq. (1) is both difficult and impractical, especially when one is interested in nonlinear spectroscopies such as the 2-pulse and 3-pulse stimulated photon echo since they involve 4-point correlation functions. From a practical standpoint it is essential, therefore, to approximate Eq. (1) even though the (complicated) linear response function corresponding to it can be derived (result not shown). In what follows we derive an expression for H_e which is adequate for $r \gtrsim 0.7$ (without a loss generality we take $\omega' < \omega''$).

Our approach involves a first-order Taylor series expansion of the $r^2 - 1$ and r^2 terms in Eq. (2) about $r = 1$ (e.g., $r^2 - 1 \approx 2r - 1$). When it is recognized that H_g of Eq. (3) is exactly equivalent to

$$H_g = \hbar\omega'(a^+ a + 1/2) - \hbar\omega''(r-1)a^+ a - \hbar\omega''(r-1)/2, \tag{4}$$

it follows easily that

$$H_e \approx \hbar\omega'\left[\left(a^+ a + \frac{1}{2}\right) + (2 - r^{-1})d(a^+ + a)/\sqrt{2} + (2 - r^{-1})d^2/2\right] + \hbar\Omega, \tag{5}$$

when the term $2^{-1}\hbar\omega'(1 - r^{-1})(a^{+2} + a^2)$ is dropped. It is the elimination of this term that leads to the desired simplification. The $(a^{+2} + a^2)$ operator brings intensity, in first order, to phononic transitions for which the quantum number n changes by ± 2. However, the contributions from that operator to such transitions which carry sufficient intensity from linear coupling to be relevant to linear and nonlinear optical experiments are small for $r \gtrsim 0.7$. The effect of the $(a^{+2} + a^2)$ operator on transitions for which the quantum number change is odd is also small for such r-values (see below for supportive results). The vertical transition frequency from Eq. (5) is

$$\Omega_v = \Omega + \omega'(2 - r^{-1})d^2/2. \tag{6}$$

The most important effect from quadratic coupling for systems of the type we are interested in has to do with the sequence structure in the absorption spectrum, i.e., $n'' = n'$ transitions which carry different frequencies, one result of which could be beats in photon echo decays. The relative intensities of such transitions depend, of course, on temperature. Importantly, the expression for H_e given by Eq. (5) retains the sequence structure. It is to be appreciated that, in general, both the effective mass and the frequency may change upon optical excitation and can contribute to the quadratic electron–photon coupling. Equation (1) assumes that only the frequency is changed. Our discussion of the limitations of Eq. (5) is based on this reference Hamiltonian. However, if the mass is allowed to change as well, these conditions may change. It is possible, for example, to find a certain ratio of mass and frequency change for which the Hamiltonian Eq. (5) is exact.

We turn next to the two-point correlation function $J(t)$ whose Fourier transform yields the linear absorption spectrum. In the Heisenberg picture,[15]

$$J(t;T) = \langle e^{iH_g t/\hbar} v(q) e^{-iH_e t/\hbar} v(q)\rho_g \rangle, \tag{7}$$

with $\rho_g = \exp(-\beta H_g)/Tr[\exp(-\beta H_g)]$, $\beta = (kT)^{-1}$. $\langle \cdots \rangle$ denotes the quantum mechanical trace (Tr) over the nuclear degrees of freedom. Because we are in the Heisenberg picture, the electronic transition dipole moment operator $v(q)$ is time-independent. In the Condon approximation, which we employ,[36] the dependence of v on the vibrational coordinates q is lost, i.e., $v(q) = v(0)$, a constant whose magnitude squared contains the square of the pure electronic transition dipole. Setting $|v(0)|^2$ multiplied by other constants equal to 1 for convenience, we are left with

$$J(t;T) = \langle e^{iH_g t/\hbar} e^{-iH_e t/\hbar} \rho_g \rangle, \tag{8}$$

to evaluate with H_g and H_e given by Eqs. (3) and (5). In doing so we employed coherent states for the phonon field rather than number states. The reader is referred to Refs. 39–42 for discussions on advantages gained in the utilization of coherent states as a complete basis set. In Appendix A we review some basic properties of coherent states, including their evolution under the time-evolution operator. We mention here only that a coherent state $|z\rangle$ is an eigenvector of the non-Hermitian lowering operator a,

$$a|z\rangle = z|z\rangle, \tag{9}$$

where the eigenvalue z can be complex, that $|z\rangle$ can be expressed as a superposition of phonon number states and that coherent states obey a special type of closure relationship:

$$\frac{1}{\pi}\int d^2 z \, \frac{|z\rangle\langle z|}{\langle z|z\rangle} = 1, \tag{10}$$

where $d^2 z = d(\mathrm{Re}\, z)d(\mathrm{Im}\, z)$. It is the elimination of the a^{+2} and a^2 operators from H_e that allows for a relatively straightforward evaluation of $J(t;T)$. The result is[43]

TABLE I. Franck–Condon factors for $S=0.8$ and $r=0.7$ and 0.8 (in parentheses).

(n',n'')[a]	Equation (17)		Exact[b]		Englman[c]	
(0,0)	0.63	(0.55)	0.51	(0.49)	0.46	(0.45)
(1,0)	0.30	(0.33)	0.40	(0.39)	0.28	(0.28)
(2,0)	0.070	(0.10)	0.091	(0.11)	0.087	(0.089)
(3,0)	0.010	(0.020)	0.0040	(0.013)	0.0200	(0.020)
(0,1)	0.29	(0.33)	0.28	(0.31)		
(1,1)	0.19	(0.088)	0.057	(0.040)		
(2,1)	0.34	(0.32)	0.43	(0.37)		
(3,1)	0.14	(0.19)	0.22	(0.24)		
(0,2)	0.066	(0.10)	0.13	(0.14)		
(1,2)	0.34	(0.32)	0.17	(0.21)		
(2,2)	0.023	(0.00020)	0.00044	(0.013)		
(3,2)	0.29	(0.21)	0.30	(0.23)		
(0,3)	0.010	(0.020)	0.053	(0.048)		
(1,3)	0.14	(0.19)	0.17	(0.19)		
(2,3)	0.29	(0.21)	0.044	(0.068)		
(3,3)	0.0035	(0.048)	0.055	(0.083)		

[a] n'' and n' are the initial and final electronic state vibrational quantum numbers. $r=\omega'/\omega''$.
[b] Calculated using MATHEMATICA with exact harmonic oscillator wavefunctions.
[c] Calculated using the equation on p. 121 of Ref. 35.

$$J(t;T)=\frac{1}{\pi}\int\frac{d^2z}{\langle z|z\rangle}\langle z|e^{iH_gt/\hbar}e^{-iH_et/\hbar}\rho_g|z\rangle \tag{11}$$

$$=\frac{C}{Q}\left(\frac{1}{f_1}\right)\exp\left[\frac{f_2}{f_1}+f_3\right], \tag{12}$$

where $Q\equiv Tr[\exp(-\beta H_g)]$ is the canonical partition function,

$$Q=[2\sinh(\beta\hbar\omega''/2)]^{-1}, \tag{13}$$

and

$$C\equiv e^{-\beta\hbar\omega''/2}e^{-i(\omega'-\omega'')t/2}e^{-i\Omega_v t}, \tag{14a}$$

$$f_1\equiv 1-e^{-\beta\hbar\omega''+i(\omega''-\omega')t}, \tag{14b}$$

$$f_2\equiv S_{eff}e^{-\beta\hbar\omega''+i\omega''t}(e^{-i\omega' t}-1)^2, \tag{14c}$$

$$f_3\equiv iS_{eff}\omega' t+S_{eff}(e^{-i\omega' t}-1). \tag{14d}$$

The derivation of Eq. (12) leads to $S_{eff}=(2-r^{-1})^2d^2/2$ which contains a term of higher order than should be retained. For this reason and because the first term of Eq. (14d) should cancel out the contribution to Ω_v from the optical reorganization energy in the last exponential of Eq. (14a), we use in what follows:

$$S_{eff}\equiv(2-r^-)d^2/2. \tag{15}$$

With this equation and Eq. (6), Eqs. (14a) and (14d) become

$$C\equiv e^{-\beta\hbar\omega''/2}e^{-i(\omega'-\omega'')t/2}e^{-i\Omega t} \tag{14a'}$$

and

$$f_3\equiv S_{eff}(e^{-i\omega' t}-1). \tag{14d'}$$

At this point it is important to establish the reliability of $J(t;T)$ as given by Eq. (12); i.e., one need check the Franck–Condon (FC) factors. The easiest way to do this is to Fourier transform $J(t;T)$ to obtain the linear absorption spectrum:

$$\sigma(\omega;T)=\frac{1}{2\pi}\int_{-\infty}^{+\infty}J(t;T)e^{i\omega t}dt. \tag{16}$$

The result is (Appendix B)

$$\sigma(\omega;T)$$
$$=2^{-1}(1-e^{-\beta\hbar\omega''})e^{-S_{eff}}\sum_{q=0}^{\infty}\frac{(S_{eff})^q}{q!}\sum_{n''=0}^{\infty}e^{-n''\beta\hbar\omega}n''!$$
$$\times\left\{\sum_{m=0}^{n''}\sum_{l=0}^{m}(-1)^{m+l}2^{-2m}\right.$$
$$\left.\times\frac{(4S_{eff})^m(2m)!\,\epsilon_l}{(m!)^2(n''-m)!(m+l)!(m-l)!}\right\}[\delta(\tilde{\omega}-l\omega')$$
$$+\delta(\tilde{\omega}+l\omega')], \tag{17}$$

where ϵ_l is the von Neumann symbol ($\epsilon_0=1$, $\epsilon_l=2$ for $l\geqslant 1$) and

$$\tilde{\omega}=\omega-\Omega-q\omega'+(\omega''-\omega')(n''+1/2). \tag{18}$$

S_{eff} is defined by Eq. (15). In Eq. (17) n'' is the initial state quantum number of the absorption transition. We performed calculations which confirmed that Eq. (17) and the numerical Fourier transform (FT) of Eq. (12) yield identical spectra. Franck–Condon factors for $n''\rightarrow n'$ transitions can be obtained from Eq. (12) by setting the value of n'' and the value of ω for the $n''\rightarrow n'$ transition of interest. One then sets the $(1-\exp(-\beta\hbar\omega''))$ and $\exp(-n''\beta\hbar\omega'')$ terms equal to unity and adds the terms in Eq. (17) whose delta functions give the correct ω-value. All appropriate delta functions are then set equal to unity. This procedure is somewhat cumbersome for hot transitions. For cold transitions, $n''=0$, it is simple because q in Eq. (17) is n' and m and l are zero. Table I compares our approximate FC factors for a few transitions with the exact FC factors calculated using harmonic oscillator wavefunctions with MATHEMATICA 2.2. [We confirmed

TABLE II. Franck–Condon factors for $S=2.0$ and $r=0.7$ and 0.8 (in parentheses).

(n',n'')[a]	Equation (17)		Exact[b]		Englman[c]	
(0,0)	0.32	(0.22)	0.19	(0.17)	0.14	(0.14)
(1,0)	0.36	(0.33)	0.37	(0.33)	0.14	(0.14)
(2,0)	0.21	(0.25)	0.30	(0.29)	0.068	(0.068)
(3,0)	0.080	(0.13)	0.12	(0.15)	0.022	(0.022)
(0,1)	0.36	(0.33)	0.26	(0.27)		
(1,1)	0.0070	(0.056)	0.077	(0.10)		
(2,1)	0.13	(0.042)	0.045	(0.017)		
(3,1)	0.24	(0.19)	0.27	(0.20)		
(0,2)	0.21	(0.25)	0.22	(0.24)		
(1,2)	0.13	(0.042)	0.0024	(0.0012)		
(2,2)	0.13	(0.17)	0.14	(0.15)		
(3,2)	0.0061	(0.016)	0.016	(0.043)		
(0,3)	0.080	(0.13)	0.15	(0.16)		
(1,3)	0.24	(0.19)	0.068	(0.077)		
(2,3)	0.0061	(0.016)	0.0610	(0.070)		
(3,3)	0.17	(0.11)	0.046	(0.040)		

[a]n'' and n' are the initial and final electronic state vibrational quantum numbers. $r=\omega'/\omega''$.
[b]Calculated using MATHEMATICA with exact harmonic oscillator wavefunctions.
[c]Calculated using the equation on p. 121 of Ref. 35.

that, for pure linear coupling, Eq. (17) gives FC factors in exact agreement with the values calculated using the latter method.] The results given in Tables I and II are for $r=0.7$ and 0.8 and $S=0.8$ (Table I) and 2.0 (Table II) with $S=d^2/2$. S_{eff} in Eq. (17) is determined using Eq. (15). Overall, the agreement between the approximate and exact FC factors may be said to be quite satisfactory. (The agreement for $r=0.8$ is better than for $r=0.7$.) As expected, the agreement for small FC factors worsens. However, the associated transitions would contribute relatively weakly to the absorption spectrum. Furthermore, for small FC factors anharmonic or even Duschinsky contributions to the intensities can be expected to be non-negligible. Also included in the tables are approximate FC factors calculated using the bottom equation on p. 121 of Englman[35] which is restricted to cold transitions. We conclude that for $r\gtrsim 0.7$, the excited state vibrational Hamiltonian given by Eq. (5) for linear and quadratic coupling is a useful approximation for condensed phase phononic transitions which contribute significantly to the absorption spectrum. Condensed phase systems which exhibit r-values smaller than 0.7 for the intermolecular modes should be rare.

B. A linear response function for a multimode system with linear electron–phonon coupling

The response function for the case of linear coupling only is obtained from Eq. (12) by setting $\omega'=\omega''$. For the multimode system,

$$J_I(t;T)=\exp[-g(t;T)], \tag{19}$$

where the lineshape function

$$g(t;T)=\sum_j g_j(t;T), \tag{20}$$

with j labeling the mode and

$$g_j(t;T)=S_j[\coth(\beta\hbar\omega_j''/2)(1-\cos(\omega_j''t)) + i\ \sin(\omega_j''t)]. \tag{21}$$

Equation (21) is a well-known result (for convenience we set the adiabatic electronic energy gap, Ω, equal to zero). Since damping is not included, the FT of $J_I(t;T)$ yields an absorption spectrum consisting of delta-function peaks; see Eq. (17). The problem, therefore, is to introduce damping(s) in a way that yields physically acceptable spectra.

The linear response and lineshape functions which follow stem from our study of the consequences of the MBO model (see Chap. 8 of Ref. 15) for linear absorption and hole-burned spectra (unpublished results). We propose a phononic contribution to $J_I(t;T)$ of the form

$$J_I^{ph}(t;T)=\exp[-g^{ph}(t;T)], \tag{22}$$

where

$$g^{ph}(t;T)=\sum_j g_j^{ph}(t;T) \tag{23}$$

and

$$g_j^{ph}(t;T)=S_j\{\coth(\beta\hbar\omega_j/2)-e^{-\gamma_j|t|/2} \times[\coth(\beta\hbar\omega_j/2)\cos(\omega_j t)-i\ \sin(\omega_j t)]\}. \tag{24}$$

Here, γ_j is the damping constant of mode j and S_j and ω_j are its Huang–Rhys factor and frequency. The FT of $\exp[-g_j^{ph}(t;T)]$ yields a delta-function line-shape for the ZPL and, for example, widths (fwhm) of $n_j'\gamma_j$ for the ''cold'' phonon transitions, $n_j''=0\rightarrow n_j'=1,...,$ *vide infra*. The linear dependence of the width on n_j' is expected for a decay mechanism of mode j that is linear in its coordinate. Let γ_{el} be the actual width of the ZPL. The response function,

$$\tilde{J}_I(t;T)=J_I^{ph}(t;T)\cdot J^{el}(t;T), \tag{25}$$

with $J_l^{ph}(t;T)$ given by Eq. (22) and

$$J^{el}(t;T)=\exp(-\gamma_{el}(T)|t|/2), \tag{26}$$

yields a ZPL with a width of γ_{el}. (We remind the reader that the temperature dependencies of γ_{el} and the γ_j's depend on the mechanisms of dephasing.) For the $n_j''=0\rightarrow n_j'=0,1...$, progression, the widths of the members are $\gamma_{el}+n_j'\gamma_j$. Clearly the addition of γ_{el} to the widths of the cold multiphonon transitions has a physical basis.

The FT of Eq. (25) for mode j is (Appendix C)

$$\begin{aligned}\sigma_j(\omega_j;T)&=\exp[-S_j\coth(\beta\hbar\omega_j/2)]\\&\times\sum_{m=-\infty}^{\infty}\sum_{l=0}^{\infty}\left\{\frac{(S_j\mathrm{cosech}(\beta\hbar\omega_j/2))^{m+2l}}{l!\Gamma(m+l+1)2^{(m+2l)}}\right.\\&\times\exp(m\beta\hbar\omega_j/2)\\&\left.\times\frac{(\gamma_{el}+(m+2l)\gamma_j)/2\pi}{(\omega-m\omega_j)^2+((\gamma_{el}+(m+2l)\gamma_j)/2)^2}\right\},\end{aligned} \tag{27}$$

where Γ is the gamma function. This equation describes the absorption spectrum associated with mode j. As expected from Eq. (24) and Eq. (26), the last term in Eq. (27) leads to Lorentzian lineshapes for all bands. Unfortunately, the complexity of Eq. (27) does not lend itself to ready visualization of the absorption spectrum. The presence of $(m+2l)\gamma_j$ in the Lorentzian suggests that there can be negative contributions to σ_j. However, the properties of the Γ function are such that $\Gamma(m+l+1)=\pm\infty$ for $(m+2l)\leqslant 0$ so that negative contributions do not arise. Figure 1 shows a spectrum calculated with Eq. (27) for $\omega_j=25\ \mathrm{cm}^{-1}$, $S_j=1.8$, $\gamma_j=3\ \mathrm{cm}^{-1}$, $\gamma_{el}=1\ \mathrm{cm}^{-1}$ and $T=50$ K. The spectrum calculated by taking the numerical FT of the response function is identical. The sharp ZPL appears superimposed on the broader (1,1) and (2,2) transitions. The effects of folding, which lead to larger widths for higher quantum number transitions, are also apparent. A further discussion of folding is given later.

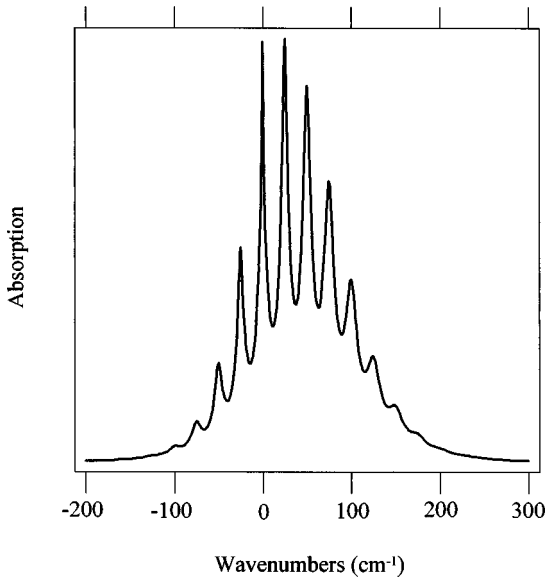

FIG. 1. Single-site absorption spectrum calculated with Eq. (27) for a model system: $\omega_j=25\ \mathrm{cm}^{-1}$; $\gamma_j=3\ \mathrm{cm}^{-1}$; $S_j=1.8$; $\gamma_{el}=1\ \mathrm{cm}^{-1}$ and $T=50$ K. The spectrum calculated by taking the numerical FT of Eq. (25) is identical.

In Appendix C we show that with $\gamma_{el}=\gamma_j=0$, one recovers the well-known frequency domain result [see, e.g., Eq. (8.43) of Ref. 15]:

$$\begin{aligned}\sigma_j(\omega;T)&=\exp\left[-S_j\coth\left(\frac{\beta\hbar\omega_j}{2}\right)\right]\\&\times\sum_{m=-\infty}^{\infty}\exp(m\beta\hbar\omega_j/2)I_m(z_0)\delta(\omega-m\omega_j),\end{aligned} \tag{28}$$

where $z_0=S_j\,\mathrm{cosech}(\beta\hbar\omega_j/2)$ and $I_m(z_0)$ are modified Bessel functions. We have also proven that[43] Eq. (27) is mathematically equivalent to Eq. (17) of Hayes *et al.*,[24] an equation whose structure is quite different than that of Eq. (27). In that paper, Eq. (17) is the basis for a frequency domain theory of hole-burned spectra. By setting $\coth(\beta\hbar\omega_j/2)=1$ in Eq. (24) and taking the FT of $\tilde{J}_l(t)$, Eq. (25), one obtains for the $T=0$ K spectrum.

$$\sigma_j(\omega)=\exp(-S_j)\sum_{m=0}^{\infty}\frac{S_j^m}{m!}\left\{\frac{(\gamma_{el}+m\gamma_j)/2\pi}{(\omega-m\omega_j)^2+((\gamma_{el}+m\gamma_j)/2)^2}\right\}, \tag{29}$$

with $\{\}$ a normalized Lorentzian with widths given by

$$(\mathrm{fwhm})_m=\gamma_{el}+m\gamma_j, \tag{30}$$

for the progression members, $m=0,1,...$. Here, the nature of the folding is clear and one has the desired result that γ_{el}, from pure electronic dephasing, adds to the widths of the multi-phonon transitions. Equation (27), with its Poisson distribution for the Franck–Condon factors, can also be obtained, starting with Eq. (27). The derivation is quite lengthy and will be given elsewhere.[43]

In summary the postulated response function $\tilde{J}_l(t;T)$ of Eq. (25), with J_l^{ph} and J^{el} defined by Eqs. (22) and (26), leads to a frequency domain expression for the absorption spectrum, Eq. (27), which yields physically reasonable spectra, as will become more apparent. Thus, single-site absorption and hole-burned spectra at finite temperature can be conveniently calculated by numerically Fourier transforming $\tilde{J}_l(t;T)$; see Sec. II D. As written, $\tilde{J}_l(t;T)$ yields Lorentzian lineshapes for all transitions. The modifications necessary to introduce different lineshapes are discussed in the final section of the paper.

C. A linear response function for a system whose modes are either linearly or quadratically coupled

As pointed out in the Introduction, there appear to be a number of systems of chromophores in amorphous solids where modes are either linearly or quadratically coupled. We consider first pure quadratic (q) coupling. The linear response function for the case of no damping is given by Eq. (12) with S_{eff} set equal to zero. Guided by the mathematical

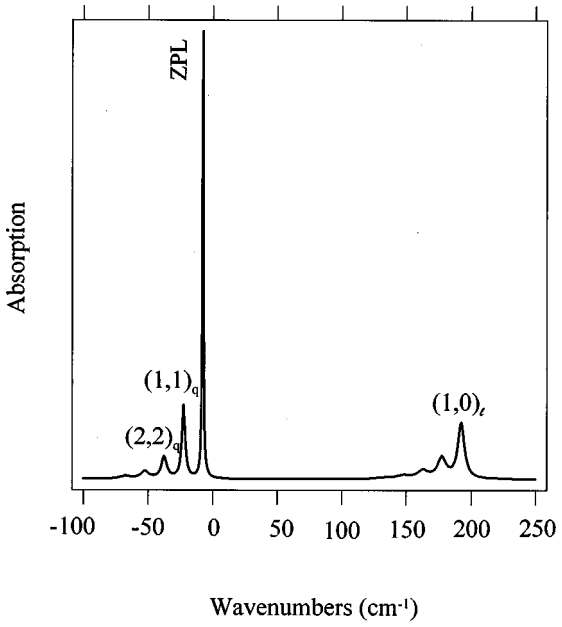

FIG. 2. Single-site absorption spectrum for $T=100$ K calculated by taking the numerical FT of Eq. (34) for a two-mode system with one mode linearly coupled (l) and the other quadratically coupled (q): $\omega_l=200\ \mathrm{cm}^{-1}$; $S_l=0.7$; $\gamma_l=5\ \mathrm{cm}^{-1}$; $\omega_q''=50\ \mathrm{cm}^{-1}$; $\omega_q''=35\ \mathrm{cm}^{-1}$; $\gamma_q=2\ \mathrm{cm}^{-1}$; and $\gamma_{el}=1\ \mathrm{cm}^{-1}$.

insights gained in the development of $\tilde{J}_l(t;T)$, Eq. (25), we were led to the following expression as a potentially useful response function which includes damping (dephasing) of the phonons and pure electronic dephasing (γ_{el}):

$$\tilde{J}_q(t;T)=J_q^{ph}(t;T)\cdot J^{el}(t;T), \tag{31a}$$

with J^{el} defined by Eq. (26) and the phononic (ph) contribution to the response function given by

$$J_q^{ph}(t;T)=\prod_j J_{q,j}^{ph}(t;T), \tag{31b}$$

with

$$J_{q,j}^{ph}(t;T)=\frac{(1-e^{-\beta\hbar\omega_j''})e^{-i(\omega_j'-\omega_j'')t/2}}{1-e^{-\beta\hbar\omega_j''-i(\omega_j'-\omega_j'')t-\gamma_j|t|/2}}. \tag{31c}$$

The FT of Eq. (31) yields a delta-function lineshape for the ZPL ($n_j''=0\rightarrow n_j'=0$ transition) and widths for the $n_j''\rightarrow n_j'=n_j''$ sequence transitions of

$$(\mathrm{fwhm})n_j''=n_j''\gamma_j;\quad n_j''=,2,..., \tag{32}$$

where γ_j is the width of the $n_j''=1\rightarrow n_j'=1$ transition. For the sake of brevity we do not give the proof of Eq. (32), but see a discussion of Fig. 2, *vide infra*. The FT of $J_{q,j}^{ph}(t;T)$ multiplied by $J^{el}(t;T)$ [Eq. (26)] yields a width of γ_{el} for the ZPL defined above. Equation (32) becomes

$$(\mathrm{fwhm})_{n_j''}=\gamma_{el}+n_j''\gamma_j;\quad n_j''=0,1,.... \tag{33}$$

With the results of this and the preceding subsection, the response function for a system whose modes are either linearly or quadratically coupled can be written as

$$\tilde{J}_{l,q}(t;T)=J_l^{ph}(t;T)\cdot J_q^{ph}(t;T)\cdot J^{el}(t;T), \tag{34}$$

with the three terms on the R.H.S. defined by Eqs. (22), (31b) and (26). Equation (34) is the main result of this paper. Figure 2 shows the absorption spectrum calculated by taking the numerical FT of Eq. (34) for a model system consisting of one linearly (l) mode and one quadratically (q) coupled mode. For the former, $\omega_l=200\ \mathrm{cm}^{-1}$, $S_l=0.7$, $\gamma_l=5\ \mathrm{cm}^{-1}$ and for the latter, $\omega_q''=50\ \mathrm{cm}^{-1}$, $\omega_q'=35\ \mathrm{cm}^{-1}$ and $\gamma_q=2\ \mathrm{cm}^{-1}$. γ_{el} is set equal to 1 cm^{-1} and $T=100$ K. The location of the ZPL at $-7.5\ \mathrm{cm}^{-1}$ is a zero-point energy effect due to the quadratically coupled mode. The width of the ZPL in Fig. 2 is 1 cm^{-1}, as expected since $\gamma_{el}=1\ \mathrm{cm}^{-1}$. The measured widths of the $(1,1)_q$ and $(2,2)_q$ sequence transitions to the left of the ZPL are 3 and 5 cm^{-1}, in accordance with Eq. (32). The cold $(1,0)_l$ transition due to the linearly coupled 200 cm^{-1} mode carries a width of 5 cm^{-1}, in accordance with Eq. (30). To the left of the $(1,0)_l$ band are the sequence transitions due to the quadratic mode. The measured width of the band to the immediate left of the $(1,0)_l$ band is 7 cm^{-1}, which is the sum of $\gamma_{el}=1\ \mathrm{cm}^{-1}$ and the phononic contributions to the widths of the $(1,1)_q$ and $(1,0)_l$ transitions.

D. Application to real systems

The lowest energy ($S_1(Q_y)\leftarrow S_0$ absorption band of the special BChl *a* pair (P) of the bacterial reaction center has been investigated in detail using hole burning spectroscopy.[29,44] For *Rb. sphaeroides* this so-called *P*-band is characterized by strong linear electron-coupling involving modes centered at $\omega_m=30\ \mathrm{cm}^{-1}$ and $\omega_{sp}=120\ \mathrm{cm}^{-1}$. The former is most likely due to protein phonons. The Huang–Rhys factor $S_m=1.8$ and the effective damping constant is $\gamma_m\sim 30-40\ \mathrm{cm}^{-1}$. In the calculations which follow a value of 20 cm^{-1} for γ_m was used in order to enhance the structure in the single-site absorption and hole-burned spectra. The 120 cm^{-1} mode is referred to as the special pair marker mode. Its effective damping constant is $\gamma_{sp}=25\ \mathrm{cm}^{-1}$ and its Huang–Rhys factor is $S_{sp}=1.5$. At sufficiently low temperatures the homogeneous width of the pure electronic transition is 5 cm^{-1} due to the 1 ps primary charge separation process that depopulates the excited state. The hole burning results indicate that the width of the ZPL remains constant at 5 cm^{-1} between 1.8 K and 15 K, at which temperature the ZPH is nearly Franck–Condon forbidden. Thus, over this temperature range the contribution to the homogeneous width of the ZPL from interaction with the bath modes is negligible.

The upper frame of Fig. 3 is the 0 K single-site absorption spectrum of the special pair calculated with Eq. (25). The parameter values given above were used. The spectrum is very similar to that calculated by Reddy *et al.*[45] in the frequency domain. The washing out of structure for the higher energy bands is due to folding. The spectrum for 15 K is shown in the bottom frame of Fig. 3. The most significant difference between the 0 K and 15 K spectra is that the ZPL of the latter is considerably weaker. This is due to a reduction in its FC factor stemming from the linearly coupled 30 cm^{-1} mode. Also, the lower frame shows a hot band at $\omega=-30\ \mathrm{cm}^{-1}$ due to (0,1) transition.

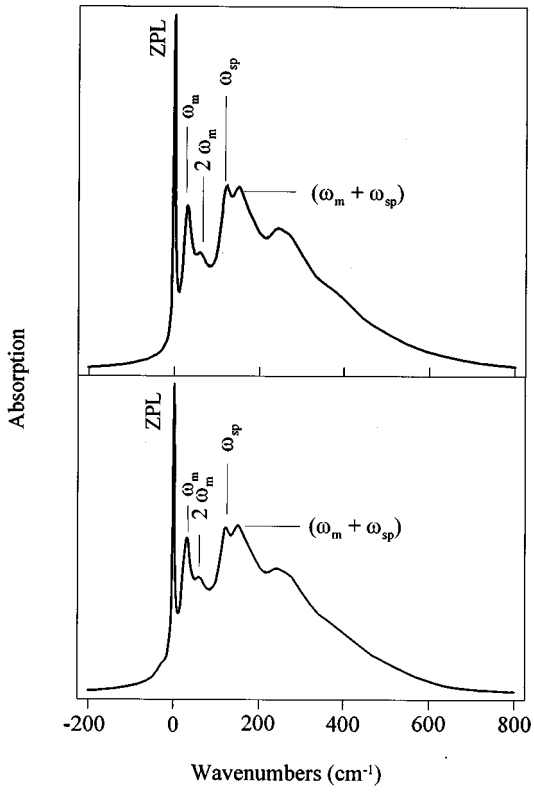

FIG. 3. Single-site absorption spectra for the special pair of the bacterial reaction center calculated with Eq. (25) at $T=0$ K (top frame) and 15 K (bottom frame) with $\omega_m=30\ \mathrm{cm}^{-1}$, $S_m=1.8$, $\gamma_m=20\ \mathrm{cm}^{-1}$, $\omega_{sp}=120\ \mathrm{cm}^{-1}$, $S_{sp}=1.5$, $\gamma_{sp}=25\ \mathrm{cm}^{-1}$ and $\gamma_{el}=5\ \mathrm{cm}^{-1}$. γ_m for the bottom frame is 15 cm^{-1}; see the text for more details.

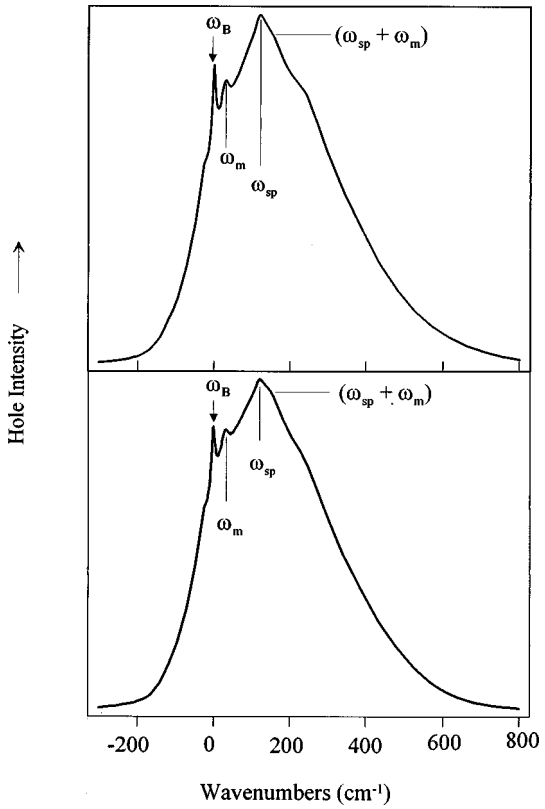

FIG. 4. Hole-burned spectra for the special pair band of the bacterial reaction center calculated with Eq. (35) for $T=0$ K (top frame) and $T=15$ K (bottom frame). $\omega=62\ \mathrm{cm}^{-1}$, $\nu_m=\omega_B=0\ \mathrm{cm}^{-1}$ and $k\tau=0.004$. Other parameter values are as given in the caption to Fig. 3.

We now extend the calculations to the hole-burned spectrum of the *P*-band. The absorption spectrum following a burn for time τ is given by[22–24]

$$\sigma_\tau(\omega;T)=\int_{-\infty}^{+\infty} d\Omega\,\chi(\Omega-\nu_m)\tilde{J}_l(\omega-\Omega) \times \exp[-k\tilde{J}_l(\omega_B-\Omega)\tau], \tag{35}$$

where Ω is the frequency of the ZPL of a single absorber and ω_B is the burn frequency. $\chi(\Omega-\nu_m)$ is a Gaussian function, with variance w^2 centered at ν_m, which governs the distribution of ZPL frequencies due to structural heterogeneity. k is the product of three terms: the absorption cross-section, the laser burn flux and the quantum yield for hole burning. $\tilde{J}_l(\omega-\Omega)$ is the absorption spectrum of a single site whose ZPL frequency is Ω. Note that for $\tau=0$, Eq. (34) is the inhomogeneously broadened absorption spectrum. The hole-burned spectrum is defined here as $\sigma_\tau(\omega;T)-\sigma_0(\omega;T)$. The 0 K (upper frame) and 15 K (lower frame) hole-burned spectra shown in Fig. 4 correspond to the single-site absorption spectra of Fig. 3. The value for the standard deviation of $\chi(\Omega-\nu_m)$ used was 64 cm^{-1} (Ref. 29) (ν_m was set equal to zero with ω_B set equal to ν_m). $k\tau$ was set at 0.004. The calculation of $\sigma_\tau(\omega;T)$ involved[46] taking the numerical Fourier transform of Eq. (25). The agreement between the 0 K hole-burned spectrum of Fig. 4 and the experimental spectrum[29] as well as the spectrum calculated using the frequency domain theory of Hayes *et al.*[24] (not shown) is good. Note the very weak intensity of the ZPH at ω_B which carries a width of $2\gamma_{el}=10\ \mathrm{cm}^{-1}$, as expected.[47] The weakness of the ZPH can be understood from its FC factor, $\overline{n}\exp[-2\{S_m(\overline{n}(\omega_m)+1)+s_{sp}(\overline{n}(\omega_{sp}+1)\}]$, where the $\overline{n}$'s are thermal occupation numbers. For $T=0$ K, the FC factor is $\exp(-6.6)=0.0014$. Elevation of the temperature to 15 K is sufficient to significantly reduce the intensity of the ZPH, in agreement with experiment.[29] The effect of increasing γ_m from 20 cm^{-1} to 40 cm^{-1}, the value used in Ref. 24, would be to significantly fill in the valley between the ZPH at ω_B and the phonon sideband hole at $\omega_B+\omega_m$, resulting in an apparent weakening of the ZPH.

As a final application we consider the chromophore APT in hyperquenched glassy films of ethanol which has been thoroughly studied by nonphotochemical hole burning spectroscopy.[17] This system is characterized by a linearly coupled mode with $\omega_l=25\ \mathrm{cm}^{-1}$, $S_l=0.5$ and $\gamma_l\sim10\ \mathrm{cm}^{-1}$ and a quadratically coupled mode with $\omega_q''=50\ \mathrm{cm}^{-1}$ which is responsible for dephasing of the zero-phonon transition. For the calculations we set $\omega_q'=35\ \mathrm{cm}^{-1}$ which represents a 30% frequency change. The temperature-dependent data of Ref. 17 indicate that $\gamma_{el}(T)=8\overline{n}(\omega_q'')\ \mathrm{cm}^{-1}$ and furthermore, that $\gamma_q(T)=5(\overline{n}(\omega_q'')+1)\ \mathrm{cm}^{-1}$ when the theoretical model of Jackson and Silbey[21] is used. γ_l is taken to be temperature independent. The single-site absorption spectra for $T=15$, 60 and 100 K shown in Fig. 5 were calculated by the numerical FT of Eq. (34). In all three spectra the ZPL is located at

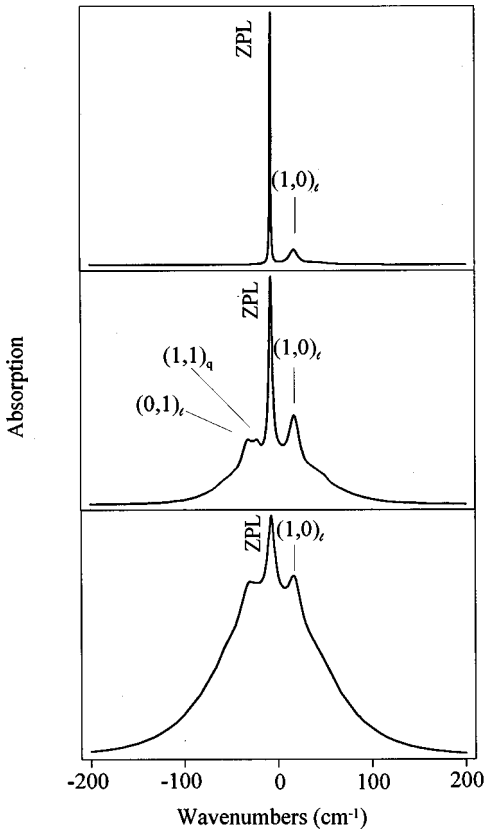

FIG. 5. Single-site absorption spectra of Al-phthalocyanine tetrasulphonate in glassy ethanol calculated by taking the numerical FT of Eq. (34) with $\omega_l=25\ \mathrm{cm}^{-1}$, $S_l=0.5$, $\gamma_l=10\ \mathrm{cm}^{-1}$, $\omega_q''=50\ \mathrm{cm}^{-1}$, $\omega_q''=35\ \mathrm{cm}^{-1}$, $\gamma_q=5(\bar{n}_q(\omega_q'')+1)\ \mathrm{cm}^{-1}$ and $\gamma_{el}=8\bar{n}_q(\omega_q'')\ \mathrm{cm}^{-1}$. The top, middle and bottom spectra are for $T=15$, 60 and 100 K, respectively.

$-(50-35)/2\ \mathrm{cm}^{-1}$ relative to $0\ \mathrm{cm}^{-1}$ which would be the position in the absence of quadratic coupling. At 15 K (top frame) only the ZPL and cold $(1,0)_l$ transition is observed. At 60 K, the sequence $(1,1)_q$ transition and hot $(0,1)_l$ transition appear as well as the $(2,0)_l$ band. The structure is diminished at 100 K (bottom frame) due to the higher probability for multi-phonon transitions and sequence transitions with larger n'' values as well as folding and the temperature dependencies imposed on γ_{el} and γ_q. At 300 K all structure is lost (the result not shown).

III. CONCLUSIONS

This paper is the result of our interest in understanding the relationship and differences between the optical coherence loss of a chromophore in a glass and in the liquid phase of the glass forming solvent.[17] Linear response functions were presented which allow for a consistent approach to the calculation of single-site and inhomogeneously broadened absorption spectra and hole-burned spectra. The response functions are appropriate for systems whose modes are underdamped. Two cases were treated: a system whose modes exhibit only linear electron–phonon coupling [Eq. (25)]; and a system whose modes are either linearly or quadratically coupled [Eq. (31a)]. The response functions take into account pure electronic dephasing, γ_{el}, which is responsible for the homogeneous width of the ZPL. Furthermore, γ_{el} adds to the widths of the multi-phonon transitions, a result which has a physical basis. As expected, the widths of the multi-phonon, sequence and combination transitions exhibit folding. The phononic contribution(s) to the response functions of Eqs. (25) and (31a) lead to folding of the widths of multi-phonon, sequence $(n_j''=n_j')$ and combination band transitions. For example, the widths of the cold multi-phonon progression, $n_j''=0\rightarrow n_j'$, are given by $\gamma_{el}+n_j'\gamma_j$, where γ_j is the damping constant for mode j. The linear dependence on the excited state mode quantum number, n_j', is expected for damping mechanisms which are linear in the coordinate q_j of mode j. Mixed crystal spectra, taken at liquid helium temperatures, have shown this dependence (see, for example, Refs. 31, 48). Mechanisms that yield such a dependence include the Duschinsky effect where, in the excited state vibrational Hamiltonian, one has q_jQ_β terms (with the Q_β's the bath coordinates), and anharmonic coupling terms that are linear in q_j. (The Duschinsky effect is actually the decay mechanism for the primary oscillators of the MBO model; see Chap. 8 of Ref. 15.)

From the properties of Fourier transforms, it follows that our response functions yield Lorentzian lineshapes for all phonon transitions. In amorphous hosts structural heterogeneity can result in a distribution of frequencies for the primary oscillators. The modification of the response functions required to take into account such inhomogeneity is straightforward. For example, if one desires Voigt profiles, one need only multiply $\exp(-\gamma_j|t|/2)$ in the response functions [see Eqs. (24) and (31c)] by $\exp(-\Delta_j^2t^2/2)$, where Δ_j^2 is the variance of the distribution of ω_j frequencies. In the limit $\gamma_j \ll \Delta_j$, the folding of the aforementioned cold multi-phonon progression carries on $(n_j')^{1/2}$-dependence, rather than an n_j-dependence.[17]

An approximate excited state vibrational Hamiltonian [H_e of Eq. (5)] which accounts for linear and quadratic electron–phonon coupling and is acceptable for mode frequency changes smaller than about 30% was derived as was the linear response function it gives rise to for the case of no damping [Eq. (12)]. Inclusion of damping for a system whose modes are both linearly and quadratically coupled results in a complex linear response function. (The complexity is far greater for the nonlinear response functions associated with photon echo spectroscopies.) Thus, we presented only the response function for a system whose modes are either linearly or quadratically coupled. Nevertheless, our approximate Hamiltonian should be useful in future studies devoted to the derivation of linear and nonlinear response functions for systems whose modes are both linearly and quadratically coupled.

As stated in the Introduction, the combination of temperature-dependent hole burning and photon echo studies above and below the glass transition of the solvent should provide new insights on optical coherence loss of chromophores in liquids. The results presented will be applied to photon echo spectroscopy in a subsequent publication.[49]

ACKNOWLEDGMENTS

Research at Iowa State University was supported by National Science Foundation (NSF) Grant No. DMR-9630781

and at the University of Rochester by grants from NSF Grants No. CHE9526125 and No. AFOSR F49620-96-1-0030.

APPENDIX A: PROPERTIES OF COHERENT STATES

Coherent states form a complete and nonorthogonal basis set. They are very useful in radiation theory and quantum optics. The coherent state $|z\rangle$ is an eigenvector of the non-Hermitian operator a. The eigenvalue equation for the vector $|z\rangle$ is

$$a|z\rangle = z|z\rangle. \tag{A1}$$

Thus z, which can be complex, is the eigenvalue of a. We can express $|z\rangle$ in terms of the number states $|n\rangle$ as

$$|z\rangle = C_0 \sum_{n=0}^{\infty} \frac{z^n}{\sqrt{n!}} |n\rangle. \tag{A2}$$

One of the most appealing properties of coherent states is that they can be chosen to be unnormalized states by setting $C_0 = 1$. Since $|n\rangle$ can be written as

$$|n\rangle = \frac{(a^+)^n}{\sqrt{n!}} |0\rangle, \tag{A3}$$

where $|0\rangle$ is the vacuum state of the oscillator, Eq. (A2) becomes

$$|z\rangle = \exp(za^+)|0\rangle. \tag{A4}$$

Applying a to Eq. (A2), one obtains

$$a|z\rangle = \sum_{n=0}^{\infty} \frac{z^n}{\sqrt{n!}} \sqrt{n}|n-1\rangle, \tag{A6}$$

$$= z \sum_{n=0}^{\infty} \frac{z^{n-1}}{\sqrt{(n-1)!}} |n-1\rangle, \tag{A7}$$

$$= z|z\rangle. \tag{A8}$$

Equations (A7) and (A8) show that $|z\rangle$ is an eigenvector of a with eigenvalue z. Coherent states lack the property of orthogonality because

$$\langle z|z'\rangle = \exp(z^* z') \neq 0. \tag{A9}$$

With Eq. (A1) one can show that

$$\exp(ca)|z\rangle = \exp(cz)|z\rangle, \tag{A10}$$

where c is a constant, while with Eq. (A4) it follows that

$$\exp(ca^+)|z\rangle - |z+c\rangle. \tag{A11}$$

Note that $\exp(ca^+)$ acts as a translational operator in coherent state space with the translational parameter c.

We now show how a^+ acts on $|z\rangle$. By taking the Hermitian conjugate of Eq. (A1), we obtain

$$|z\rangle a^+ = z^* \langle z|. \tag{A12}$$

Using Eq. (A4),

$$a^+|z\rangle = a^+ \exp(za^+)|0\rangle, \tag{A13}$$

$$= (\partial/\partial z)\exp(za^+)|0\rangle, \tag{A14}$$

$$= \partial/\partial z|z\rangle. \tag{A15}$$

Recall that $\langle z|z\rangle \neq 1$. Equation (A15) confirms that $\exp(ca^+)$ is a translational operator.

We next show how $|z\rangle$ evolves in time under the time evolution operator $\exp(-iH_g t/\hbar)$,

$$\exp(-iH_g t/\hbar)|z(0)\rangle = |z(t)\rangle. \tag{A16}$$

Using Eq. (A2) one obtains

$$\exp(-iH_g t/\hbar|z(0)\rangle$$

$$= \sum_{n=0}^{\infty} \frac{z^n}{\sqrt{n!}} \exp[-i\omega''(a^+a + 1/2)t]|n\rangle, \tag{A17}$$

$$= \exp(-i\omega''t/2) \sum_{n=0}^{\infty} \frac{z^n}{\sqrt{n!}} \exp(-in\omega''t)|n\rangle, \tag{A18}$$

$$= \exp(-i\omega''t/2) \sum_{n-0}^{\infty} \frac{[z\ \exp(-i\omega''t)]^n}{\sqrt{n!}} |n\rangle, \tag{A19}$$

$$= \exp(-i\omega''t/2)|\exp(-i\omega''t)z(0)\rangle, \tag{A20}$$

$$= |z(t)\rangle. \tag{A21}$$

To operate with $\exp(-iH_e t/\hbar)$ on $|z(0)\rangle$, one of the following approaches may be used: Feynman's formula for noncommuting exponential operators,[50] Lie algebra for disentangling noncommuting exponential operators,[30] or the Inverse Campbell–Baker–Hausdorff formula (Zassenhause formula).[51–53] All three approaches worked equally well when we eliminated the a^2 and a^{+2} operators in H_e. The Lie algebra approach was found to be straightforward for pure quadratic coupling. We found that using the Zassenhause formula without eliminating a^2 and a^{+2} led to an unrecognized pattern of infinite terms which we were not able to simplify.

APPENDIX B: DERIVATION OF EQUATION 17

Here we provide a derivation of Eq. (17) starting with Eq. (12). We define $\alpha_1 \equiv \exp(f_3)$ [f_3 is given in Eq. (14d)], upon power series expansion we obtain

$$\alpha_1 = \exp(-S_{eff}) \sum_{q=0}^{\infty} \frac{(S_{eff} e^{-i\omega' t})^q}{q!}. \tag{B1}$$

We have

$$\frac{C}{Q}\left(\frac{1}{f_1}\right) = \frac{e^{-i\Omega t} e^{-i(\omega' - \omega'')t/2}(1 - e^{-\beta\hbar\omega''})}{1 - e^{-\beta\hbar\omega'' + i(\omega'' - \omega')t}}, \tag{B2}$$

where Ω is the adiabatic gap and, from Eq. (13),

$$Q = [2\sinh(\beta\hbar\omega''/2)]^{-1}$$

$$= \exp(-\beta\hbar\omega''/2) \cdot [1 - \exp(-\beta\hbar\omega'')]^{-1}.$$

For notational simplicity we define

$$f_2 = S_{eff} e^{-\beta\hbar\omega'' + i\omega'' t}(e^{-i\omega' t} - 1)^2 \equiv -\alpha_2 \alpha, \tag{B3}$$

where $\alpha_2 \equiv -S_{eff} e^{i\omega' t}(e^{-i\omega' t}-1)^2$ and $\alpha \equiv e^{-\beta\hbar\omega'' + i\omega'' t - i\omega' t}$. With Eqs. (B1)–(B3), $J(t)$ becomes

$$J(t) = \frac{C}{Q}\,\alpha_1\,\frac{1}{1-\alpha}\exp\left[-\frac{\alpha_2\alpha}{1-\alpha}\right]. \tag{B4}$$

With $J(t)$ in this form, one can utilize the generating function for Laguerre polynomials:

$$\exp[-\alpha_2\alpha/(1-\alpha)]\left(\frac{1}{1-\alpha}\right) = \sum_{n''=0}^{\infty} \mathscr{L}_{n''}(\alpha_2)\alpha^{n''}. \tag{B5}$$

With Eq. (B5), $J(t)$ becomes

$$J(t) = \frac{C}{Q}\exp(-S_{eff}) \times \sum_{q=0}^{\infty} \frac{(S_{eff}e^{-i\omega' t})^q}{q!} \sum_{n''=0}^{\infty} \mathscr{L}_{n''}(\alpha_2)\alpha^{n''}. \tag{B6}$$

Equation (B6) needs further simplification which can be accomplished by noting that $\alpha_2 = 4S_{eff}\sin^2(\omega' t/2)$ and $\mathscr{L}_{n''}(\alpha_2)$ can be rewritten as

$$\mathscr{L}_{n''}(\alpha_2) = \sum_{m=0}^{n''} (-1)^m \binom{n''}{n''-m} \frac{\alpha_2^m}{m!}. \tag{B7}$$

$J(t)$ can now be written as

$$J(t) = \frac{C}{Q}\exp(-S_{eff}) \sum_{q=0}^{\infty}\sum_{n''=0}^{\infty} \frac{(S_{eff}e^{-i\omega' t})^q}{q!} \times \left\{\sum_{m=0}^{n''} (-1)^m \binom{n''}{n''-m} \frac{[4S_{eff}\sin^2(\omega' t/2)]^m}{m!}\right\}\alpha^{n''}, \tag{B8}$$

The $[\sin(\omega' t/2)]^{2m}$ factor can be dealt with using the following identity:

$$\sin(\omega' t/2)^{2m} = 2^{-2m}(2m)!\sum_{l=0}^{m} \frac{(-1)^l \epsilon_l \cos(2l\omega' t/2)}{(m+l)!(m-l)!}. \tag{B9}$$

Equations (B8) and (B9) lead directly to Eq. (17) via a straightforward Fourier transform.

APPENDIX C: DERIVATION OF EQUATIONS 27 AND 28

In this appendix we show the derivation of Eq. (27) and the recovery of Eq. (28). $\tilde{J}_l(t;T)$ for one mode is ($\Omega = 0$)

$$\tilde{J}_l(t;T) = \exp\{-\gamma_{el}|t|/2 - S_j\coth(\beta\hbar\omega_j/2) + S_j e^{-\gamma_j|t|/2}[\coth(\beta\hbar\omega_j/2)\cos(\omega_j t) - i\sin(\omega_j t)]\}, \tag{C1}$$

which can be rewritten as

$$\tilde{J}_l(t;T) = \exp[-\gamma_{el}|t|/2 - S_j\coth(\beta\hbar\omega_j/2)] \times \exp\{S_j e^{-\gamma_j|t|/2}\sqrt{\coth^2(\beta\hbar\omega_j/2)-1}\cos(\omega_j t - \varphi_j)\}. \tag{C2}$$

Here

$$\varphi_j = \arctan\left(\frac{-i}{\coth(\beta\hbar\omega_j/2)}\right) = -i\beta\hbar\omega_j/2. \tag{C3}$$

To proceed further, one needs to decompose Eq. (C2) by using the generating function for modified Bessel functions,

$$\tilde{J}_l(t;T) = \exp[-\gamma_{el}|t|/2 - S_j\coth(\beta\hbar\omega_j/2)] \times \sum_{m=-\infty}^{\infty}\{I_m(S_j\,\mathrm{cosech}(\beta\hbar\omega_j/2)e^{-\gamma_j|t|/2}) \times \exp(im\omega_j t - m\beta\hbar\omega_j/2)\}. \tag{C4}$$

The time-dependent argument of I_m makes Fourier transform very difficult. However, this is dealt with by using the definition of $I_m(W_j)$:

$$I_m(W_j) = \sum_{l=0}^{\infty} \frac{(W_j/2)^{m+2l}}{l!\Gamma(m+l+1)}, \tag{C5}$$

where

$$W_j \equiv S_j\,\mathrm{cosech}(\beta\hbar\omega_j/2)e^{-\gamma_j|t|/2}. \tag{C6}$$

Substitution of Eq. (C5) into Eq. (C4) results in

$$\tilde{J}_l(t,T) = \exp[-S_j\coth(\beta\hbar\omega_j/2)] \times \sum_{m=-\infty}^{\infty}\sum_{l=0}^{\infty} \frac{[S_j\,\mathrm{cosech}(\beta\hbar\omega_j/2)]^{m+2l}}{2^{m+2l}l!\Gamma(m+l+1)} \times \exp(m\beta\hbar\omega_j/2)\exp[-im\omega_j t - ((m+2l)\gamma_j + \gamma_{el})|t|/2]. \tag{C7}$$

The Fourier transform of Eq. (C7) leads directly to Eq. (27). Note that we have switched the signs in $\exp(im\omega_j t - m\beta\hbar\omega_j/2)$ so that the high and low energy sides of the spectrum relative to the ZPL have positive and negative energies, respectively.

Finally, Eq. (28) is obtained from Eq. (C4) by setting $\gamma_{el} = \gamma_j = 0$:

$$J_l(t;T) = \exp[-S_j\coth(\beta\hbar\omega_j/2)]\sum_{m=-\infty}^{\infty} e^{m\beta\hbar\omega_j/2} \times I_m[S_j\,\mathrm{cosech}(\beta\hbar\omega_j/2)]\exp(-im\omega_j t). \tag{C8}$$

The straightforward Fourier transformation of Eq. (C8) leads directly to Eq. (28).

[1] Y. J. Yan and S. Mukamel, J. Chem. Phys. **94**, 179 (1991).
[2] W. B. Bosma, Y. J. Yan, and S. Mukamel, Phys. Rev. A **42**, 6920 (1990).
[3] M. Cho and G. R. Fleming, J. Chem. Phys. **98**, 2848 (1993).
[4] P. Vöhringer, D. C. Arnett, R. A. Westervelt, M. J. Feldstein, and N. F. Scherer, J. Chem. Phys. **102**, 4027 (1995).
[5] M. S. Pshenichnikov, K. Duppen, and D. A. Wiersma, Phys. Rev. Lett. **74**, 674 (1995).

[6] W. P. de Boeij, M. S. Pshenichnikov, K. Duppen, and D. A. Wiersma, Chem. Phys. Lett. **138**, 1 (1995).
[7] T. Joo, Y. Jia, J-Y. Yu, M. J. Lang, and G. R. Fleming, J. Chem. Phys. **104**, 6089 (1996).
[8] G. R. Fleming and M. Cho, Annu. Rev. Phys. Chem. **47**, 109 (1996).
[9] C. H. B. Cruz, R. L. Frork, W. H. Knox, and C. V. Shank, Chem. Phys. Lett. **132**, 341 (1986).
[10] W. P. de Boeij, M. S. Pshenichnikov, and D. A. Wiersma, J. Phys. Chem. **100**, 11806 (1996).
[11] P. Vöhringer, D. C. Arnett, T.-S. Yang, and N. F. Scherer, Chem. Phys. Lett. **237**, 387 (1995).
[12] C. J. Bardeen and C. V. Shank, Chem. Phys. Lett. **226**, 310 (1994).
[13] Y. J. Yan and S. Mukamel, Phys. Rev. A **41**, 6485 (1990); J. Chem. Phys. **94**, 179 (1991).
[14] S. Mukamel, Annu. Rev. Phys. Chem. **41**, 647 (1990); Adv. Chem. Phys. **70**, 165 (1988).
[15] S. Mukamel, *Principles of Nonlinear Optical Spectroscopy* (Oxford University Press, New York, 1995).
[16] T. Reinot, W.-H. Kim, J. M. Hayes, and G. J. Small, J. Chem. Phys. **104**, 793 (1996).
[17] T. Reinot, W.-H. Kim, J. M. Hayes, and G. J. Small, J. Chem. Phys. **106**, 457 (1997).
[18] R. Jankowiak, J. M. Hayes, and G. J. Small, Chem. Rev. **93**, 1471 (1993).
[19] L. R. Narashiman, K. A. Littau, D. W. Pack, Y. S. Bai, A. Elschner, and M. D. Fayer, Chem. Rev. **90**, 439 (1990).
[20] R. M. Shelby, C. B. Harris, and P. A. Cornelius, J. Chem. Phys. **70**, 34 (1979).
[21] B. Jackson and R. Silbey, Chem. Phys. Lett. **99**, 331 (1983).
[22] J. M. Hayes and G. J. Small, J. Phys. Chem. **90**, 4928 (1986).
[23] R. Jankowiak, J. M. Hayes, and G. J. Small, Chem. Rev. **93**, 1471 (1993).
[24] J. M. Hayes, P. A. Lyle, and G. J. Small, J. Phys. Chem. **98**, 7337 (1994).
[25] Y. Nagasawa, S. A. Passino, T. Joo, and G. R. Fleming, J. Chem. Phys. **106**, 4840 (1997).
[26] C. J. Bardeen, G. Cerullo, and C. V. Shank, Chem. Phys. Lett. **280**, 127 (1997).
[27] An extensive review of low temperature absorption spectra of chromophore in host crystals and hole-burned and fluorescence line narrowed of chromophores in amorphous hosts and proteins failed to reveal a clear cut case of overdamping. We note that the damping constants for the 50 and 180 cm^{-1} acoustic modes which dephase the pure electronic transition of APT in annealed glassy water correspond to widths of 17 and 15 cm^{-1}, respectively, at the glass transition temperature of 135 K.
[28] G. J. Small, J. Chem. Phys. **54**, 3300 (1971).
[29] P. A. Lyle, S. V. Kolaczkowski, and G. J. Small, J. Phys. Chem. **97**, 6924 (1993).
[30] F. M. Fernández and E. A. Castro, *Algebraic Methods in Quantum Chemistry and Physics* (CRC Press, Boca Raton, FL, 1995).
[31] R. L. Beckman and G. J. Small, Chem. Phys. **30**, 19 (1978).
[32] C. Manneback, Physica A **17**, 1001 (1951).
[33] M. G. Prais, D. F. Heller, and K. F. Freed, Chem. Phys. **6**, 331 (1974).
[34] D. F. Heller, K. F. Freed, and W. M. Gelbart, J. Chem. Phys. **56**, 2309 (1972).
[35] R. Englman, *Non-Radiative Decay of Ions and Molecules In Solids* (North-Holland, Amsterdam, 1979).
[36] See Refs. 37 and 38 for an approach to evaluation of Eq. (7) with $v(q)$ expressed as $v_0 \exp(cq)$ where c and v_0 are constants.
[37] Y. Tanimura and S. Mukamel, J. Opt. Soc. Am. B **10**, 2263 (1993).
[38] V. Khidekel and S. Mukamel, Chem. Phys. Lett. **240**, 304 (1995).
[39] R. J. Glauber, Phys. Rev. **131**, 2766 (1963).
[40] J. R. Clauder and B-S. Skagerstam, *Coherent States—Applications in Physics and Mathematical Physics* (World Scientific, Singapore, 1985).
[41] M. Weissbluth, Photon–Atom Interactions (Academic, New York, 1989).
[42] W. H. Louisell, *Quantum Statistical Properties of Radiation* (Wiley, New York, 1973).
[43] M. Toutounji, Ph.D. dissertation, Iowa State University, 1998.
[44] G. Small, Chem. Phys. **197**, 239 (1995), and references therein.
[45] N. R. S. Reddy, P. A. Lyle, and G. J. Small, Photosyn. Res. **31**, 167 (1992).
[46] A MATHEMATICA program has been written such that the numerical FT of $\tilde{J}_I(t,T)$ was maintained in unevaluated form as a function of ω (via the set delay operator built into MATHEMATICA). Then the program was instructed to substitute the evaluated numerical transform as a function of $\omega-\Omega$ or $\omega_B-\Omega$ in Eq. (35). The numerical integration was performed 1101 times to cover the frequency range shown in Fig. 4.
[47] *Persistent Spectral Hole Burning, Science and Applications*, edited by W. E. Moerner (Springer-Verlag, New York, 1987), Vol. 44.
[48] G. Fischer, Chem. Phys. Lett. **20**, 569 (1973).
[49] M. Toutounji, S. Mukamel, and G. J. Small, J. Chem. Phys. (submitted).
[50] R. P. Feynman, Phys. Rev. **84**, 108 (1951).
[51] W. Magnus, Commun. Pure Appl. Math. **7**, 649 (1954).
[52] R. M. Wilcox, J. Math. Phys. **8**, 962 (1967).
[53] M. Suzuki, Commun. Math. Phys. **57**, 193 (1977).